Research Article / Araştırma Makalesi GU J Sci, Part A, 9(3): 225-232 (2022) https://doi.org/10.54287/gujsa.1134881

Gazi University
Journal of Science
PART A: ENGINEERING AND INNOVATION
http://dergipark.org.tr/gujsa

The Effect of Nanostructured Titanium Surface on Protein Adsorption

Hasret Tolga ŞİRİN[1*], Ebru AKDOĞAN[1]

[1]*Ankara Hacı Bayram Veli Üniversitesi, Kimya Bölümü, Polatlı, 06900, Türkiye*

Keywords

Titanium Implant
Nanotube
Anodic Oxidation
Protein
Protein Adsorption

Abstract

The amount and conformation of bovine serum albumin upon adsorption on titanium (Ti) surfaces containing nanotubes with different pore sizes were investigated. Nanotubes were created on the surfaces via anodization. Protein adsorption behavior on anodized surfaces were compared with the adsorption behavior on smooth and sanded Ti surfaces. The conformational changes in surface adsorbed proteins were evaluated using the second derivative and curve fitting methods applied to the Fourier transform infrared spectra of the surfaces. Results showed that the amount of protein adsorbed on the surfaces increased significantly with increasing surface roughness and a significant change in the conformation of the adsorbed protein occurred on every surface albeit in a different fashion. When anodized samples were considered, it was observed that the changes in the secondary structure seemed to be correlated with to the pore size of the nanotubes rather than the surface roughness.

Cite

Şirin, H.T., & Akdoğan E. (2022). The Effect of Nanostructured Titanium Surface on Protein Adsorption. *GU J Sci, Part A, 9*(3), 225-232.

Author ID (ORCID Number)

H. T. Şirin, 0000-0002-5850-3052
E. Akdoğan, 0000-0002-1388-5595

Article Process

Submission Date 23.06.2022
Revision Date 10.08.2022
Accepted Date 16.09.2022
Published Date 26.09.2022

1. INTRODUCTION

For many years, titanium (Ti) and its alloys are being used in hard tissue repair due to their good biological compatibility and mechanical properties. The roughness of the Ti implant surface is one of the most important factors affecting the bond between the bone and the implant (Sirin et al., 2016). The current trend in Ti biomaterials research is to develop surfaces with nanoscale topographic properties manipulate in vivo tissue response at the biomolecular and cellular level. The nano-topography of the surface determines the binding of important molecules in the blood, such as proteins, to the surface. Since the in vivo response to surface nano-topography at the cellular level is directed by the initial layer of surface adsorbed proteins, the design of biomaterial surfaces needs to consider optimizing protein adsorption and conformation (Lord et al., 2010).

The protein adsorption behavior, that can be defined as both the amount and the conformation of the surface bound proteins is a complex phenomenon affected by the physiochemical properties of the surface and the surrounding environment and the nature of the protein (Chen et al., 2022). Some of these effects, such as hydrophobic surfaces inducing more protein adsorption and protein denaturation, proteins adsorbing to surfaces at higher amounts when they are close to their isoelectric points, or protein adsorption being hampered when the surface and the protein bear the same charge due to electrostatic repulsions, have been extensively studied and widely elucidated (Barberi & Spriano, 2021). However, understanding the effect of surface nanonopography is an ongoing research interest. It is usually accepted that increased roughness affects protein-surface interactions by providing increased surface area and enhanced wettability (Barberi & Spriano, 2021). The surface nanotopography can dramatically change the protein adsorption behavior (Hu et al., 2022). For example, although the surface wettability is generally accepted as being correlated with protein adsorption and hydrophobic surfaces are shown to induce more protein adsorption and protein denaturation, for Ti surfaces,

*Corresponding Author, e-mail: tolga.sirin@hbv.edu.tr

it was reported that this correlation is valid for smooth Ti surfaces with rms roughness values lower than 1 nm. When the surface become rougher this correlation no longer holds (*Sq*>5nm) (Barberi & Spriano, 2021). The protein conformation is also reported to significantly affected by nanomaterials. For example, a specific nanostructure such as nanowires can modulate protein conformation as to promote osteogenic differentiation better than other nanostructures (Li et al., 2020), the same nano-morphology can have a different effect on the adsorption behavior of different proteins (Yang et al., 2021). The conformation of proteins on TiO_2 nanotube arrays are reported to have a more critical role in subsequent cellular response and the conformation of a model protein fibronectin is reported to be determined by pore size of the arrays (Qi et al., 2021; Wu et al., 2022). Nano sized metal-organic frameworks have been reported to induce more vigorous conformational changes on the structure of human serum albumin than micro sized metal-organic frameworks (Gan et al., 2022).

In this study we aimed to investigate how nanostructures formed on Ti surface affects the amount and the conformation of surface adsorbed protein. For this purpose, surface nano structures were created in the form of nanotubes by anodic oxidation. The amount of protein (bovine serum albumin, BSA) adsorption on smooth, sanded and nanotube containing Ti surfaces as well as the changes in its conformation upon surface adsorption were compared. The significance of this study is that the results supports the paradigm that the protein adsorption behavior is dependent on nano-morphological features other than the surface roughness.

2. MATERIAL AND METHOD

2.1. Sample Preparation

Ti plates, cut into 1x2 cm dimensions, were cleaned sequentially in liquid detergent solution and 70% ethyl alcohol (Merck KGaA, Germany) by sonication (Elma GmbH, Germany). To remove the protective and inactive amorphous oxide layer on the surface Ti was etched in a 2% (v/v) HF (Merck KGaA, Germany); 3% (v/v) HNO3 (Merck KGaA, Germany) solution under a fume hood for 5 minutes and washed with deionized water and left to dry in an oven at 70°C (Jeio Tech, Korea).

2.2. Anodic Oxidation and Sanding

Anodizing setup consisted of a DC power supply (Micro Medical Electronics, Turkey), Ti (anode) connected to the positive end of the source, platinum (cathode) connected to the negative end of the source, an electrolyte solution and a magnetic stirrer (Isotex, China) where the distance between the anode and cathode was kept constant at 4 cm. Ethylene glycol (Merck KGaA, Germany) containing 0.1M NH_4F (Merck KGaA, Germany) was used as electrolyte. Anodization processes were conducted at 20, 40, and 60 V for 20 minutes. After the process, the samples were rinsed with deionized water and dried at 70 °C. Sanded Ti plates (SB) were prepared using polishing papers. Samples were sanded with silicon carbide papers (3M), (P600, P1000, P2000, P2500, P3000), cut into pieces with 1x2 cm dimensions and cleaned sequentially in liquid detergent solution and 70% ethyl alcohol by sonication for 5 minutes. Finally, the samples were rinsed with deionized water and dried at 70°C.

2.3. Surface Characterization

Surface morphologies were evaluated using scanning electron microscope (TESCAN GAIA3 FIB-SEM)). The pore size and pore distribution of the TiO_2 nanotube arrays were analyzed using ImageJ program (1.53q) on the plan view of the surface. The morphology of the surfaces was investigated using atomic force microscopy (AFM, XE-100E, PSIA, South Korea) over an area of 1μm x 1μm in tapping mode using. Mean roughness (Ra) value was calculated using the Gwyddion software (Gwyddion 2.60). The wettability of the surfaces was determined in terms of water contact angle (WCA) by an optical tensiometer (Attension Theta, Biolin Scientific, Sweden). The sessile drop method was used for this purpose.

2.4. Protein Adsorption

The amount of protein adsorption on the samples was determined using BSA (Serva Electrophoresis GmbH, Germany) as the model protein. For this purpose, samples were kept at 37°C for 24 hours in 1 mg/mL BSA solution in pH 7.4 phosphate buffered saline using a shaking water bath after which material surfaces were washed with the buffer solution for removing non-adsorbed proteins. Surface adsorbed proteins were extracted

using 1% sodium dodecyl sulfate (SDS, Merck KGaA, Germany) solution and its amount was determined using the bicinchoninic acid analysis (micro BCA, Thermo Scientific, USA), following the protocol included in the kit. Absorbance measurements were performed at a wavelength of 562 nm in a microplate reader (BMG LABTECH, Germany).

2.5. Protein Conformation

The spectra of protein adsorbed Ti surfaces were taken by averaging 512 scans for each sample using an attenuated total reflectance Fourier transform infrared spectrophotometer (FTIR-ATR, Bruker, USA) at a resolution of 4 cm^{-1}. A diamond crystal tip was used for the collection of the spectra. Following baseline correction, the amide-I band was further analyzed using the OriginPro software (Origin Lab, USA). The spectra were smoothed with 7-9 points Savitzky-Golay, the location of the component bands was determined from the second derivative of the spectra, and the component band positions and relative areas were determined using the curve fitting method. A Gaussian band shape was assumed and the band positions were not fixed during curve fitting (Akdoğan & Mutlu, 2012).

2.6. Statistical Analysis

For all measurements at least three samples were used (n=3) and the results are given as mean ± standard deviation. Protein adsorption data were evaluated using one-way ANOVA and pairwise comparisons were made using Tukey's test at the 99.5% confidence level.

3. RESULTS AND DISCUSSION

3.1. Surface Characterization

SEM images of the anodized samples (Figure 1) confirmed nanotube formation on Ti surfaces. The pore diameter increased with increasing processing voltage and the Feret pore diameters of the nanotubes were calculated as 53 ± 23 nm, 62 ± 33 nm and 125 ± 17 nm for 20V, 40V and 60V samples, respectively.

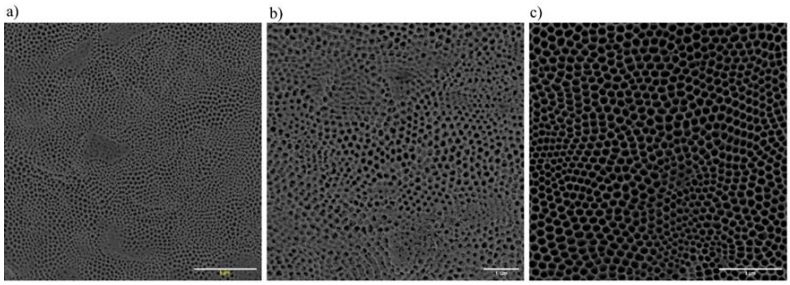

Figure 1. *SEM images of anodized Ti surfaces at 50kX magnification* ***a)*** *20V,* ***b)*** *40V and* ***c)*** *60V*

The average roughness values (Ra) of the surfaces calculated from AFM images (Figure 2) were 7.04 nm, 13.91 nm, 16.21 nm, 18.30 nm and 18.89 nm for Ti, SB, 20V, 40V and 60V samples, respectively. Ti surface, is smoother than other surfaces, and both sanding and anodization processes increased the roughness of the surfaces. The surface roughness increased with the increasing applied voltage and this increase was more pronounced between the 20V and 40V sample surfaces than between the 40V and 60V sample surfaces.

The WCA values for Ti, SB, 20V, 40V and 60V were calculated as 78° ± 3°, 66° ± 1°, 37° ± 6°, 34° ± 2° and 30° ± 2°, respectively. Although sanding increased the surface roughness, it only partially improved the surface wettability, while the effect of anodization process on WCA was more noticeable. Surface wettability determines the type interaction between the protein and the surface so that the hydrophobic interactions are dominant between proteins and hydrophobic surfaces, and electrostatic and van der Waals interactions are dominant between proteins and hydrophilic surfaces. In addition, surface hydrophilicity also affects the protein conformation such that protein denaturation becomes more significant as the hydrophobicity increased (Barberi & Spriano, 2021).

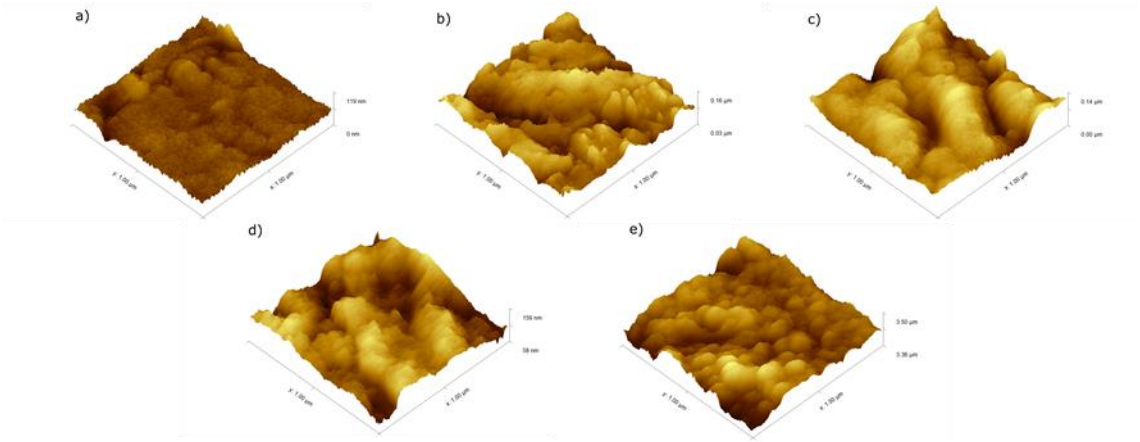

Figure 2. *3D AFM images of* ***a)*** *Ti,* ***b)*** *SB,* ***c)*** *20V,* ***d)*** *40V and* ***e)*** *60V samples*

3.2. Protein Adsorption

The amount of BSA adsorbed on Ti, SB, 20V, 40V and 60 V surfaces were; 295.59 ± 34.6 µg/cm2, 368.03 ± 29.34 µg/cm2, 387.76 ±15.13 µg/cm2, 401.33 ±22.68 µg/cm2 and 488.41 ±14.85 µg/cm2 respectively (Figure 3). However, the difference between the amount of BSA adsorbed on the SB, 20V and 40V sample surfaces at the 95% confidence level was not significant. With a hydrodynamic diameter of 7.2 nm, BSA can enter into nano-pores larger than 9 nm and can be adsorbed there, as the pores gets larger, more than one BSA molecule can be absorbed without significantly affecting each other's conformation. Hence, increased porosity in such surfaces is reported to be the main reason for an increased amount of protein adsorption (Singh et al., 2011, Liu et al., 2016). The pore sizes of all anodized samples are well over 9 nm and the increased amount of surface adsorbed protein compared to the Ti surface can be attributed to the increased porosity. In the literature, contradictory results have been reported as how sanding process affects protein adsorption concluding that random roughness provided by this process either increases or does not significantly affect the protein adsorption (Barberi & Spriano, 2021). In this study, the roughness obtained at Ra 13.9 nm level with sanding significantly increased BSA adsorption compared to the relatively smoother Ti surface. The fact that there is no dramatic difference between the WCA values of these two surfaces indicates that the increased surface area might be responsible for the increase in the amount of surface adsorbed protein.

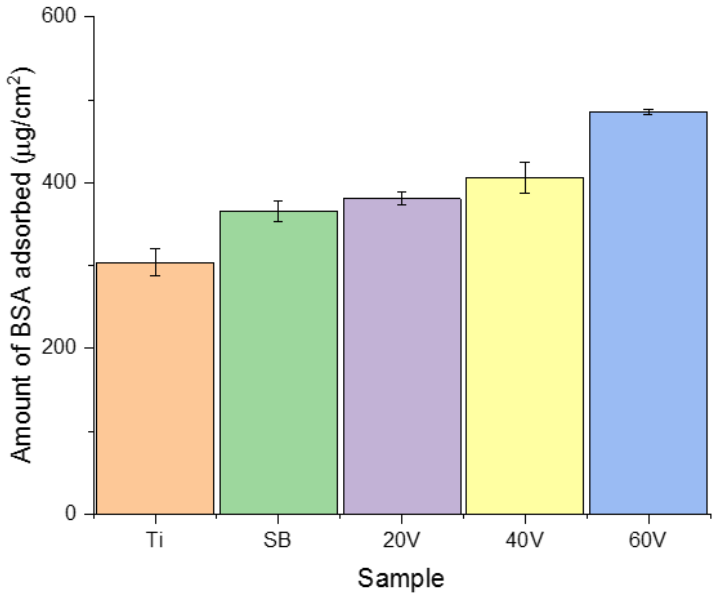

Figure 3. *Comparison of the amount of BSA adsorbed on Ti, SB, 20V, 40V and 60V samples*

3.3. Protein Conformation

Figure 4 represents the changes in the adsorbed BSA's secondary structure that were evaluated using amide-I band components. The side chain vibrations of tyrosine and arginine amino acids observed between 1611-1617 cm^{-1} were not included in the calculations. The bands corresponding to α-helix are positioned between 1649-1658 cm^{-1}, and the bands corresponding to random coils are positioned between 1641-1650 cm^{-1} (Byler & Susi, 1986; Akdoğan & Mutlu, 2012). It is not always straightforward to distinguish between these two components since their respective wavelengths are close and spectral artifacts arising from water vapor can affect the second derivative spectrum of the amide-I band and BSA is known to contain both components. Therefore, it can be accepted that the component bands between 1646-1650 cm^{-1} represent both α-helix and irregular structures (Giacomelli et al., 1999). Component bands observed between 1623-1630 cm^{-1} and 1669-1690 cm^{-1} were attributed to the β-sheet and β-turns, respectively (Byler & Susi, 1986; Giacomelli et al., 1999, Akdoğan & Mutlu, 2012). Amide-I band components for adsorbed BSA were calculated based on these band positions (Table 1). BSA gives maxima around 1655 cm^{-1} in solution, when adsorbed on the Ti surface, the maxima were observed at a wavelength close to this value, at 1657 cm^{-1}. The amide-I maxima was significantly shifted to lower wavelengths for BSA adsorbed on other sample surfaces suggesting a notable reduction in the α-helix structure. The data presented in Table 1 show that BSA undergoes significant conformational changes as a result of surface adsorption on all surfaces. The ratio of α-helix and random coil structure increased for BSA adsorbed on SB, 20V, 40V and 60V surfaces. The amide-I maxima shifted to 1647-1651 cm^{-1}, which indicates a decrease in the α-helix content of BSA but an increase in its random coil content. The β-layer content of BSA's secondary structure on the 60V surface increased dramatically. The α-helix and random coil contents tended to increase as the Ra value increased for 20V and 40V samples. However, despite an increase in Ra value for the 60V sample, the α-helix and random structure content deviates from this trend and decreases instead while the β-layer content increases significantly. It has been reported that a protein having a natural tendency to form helix structures can acquire secondary structure rich in β structures depending on the changes in ambient conditions, and the content of regular β structures can even reach up to 75% and form amyloid-like aggregates (Della Porta et al., 2016). When the anodized samples are compared it can be observed that both the Feret pore diameter and surface roughness increased somewhat proportionally for 20V and 40V samples, but the pore diameter on the 60V sample increased almost 2 times compared to that of the 40V sample. The α-helix and random coil content of BSA adsorbed on the surfaces increased with increasing surface roughness up to a certain pore size, but such a conclusion cannot be made for β-sheet and β-turn contents. It is also important to note that the average pore size obtained on all anodized samples was greater than the dimensions of BSA (15x4x4 nm) (La Verde et al., 2017).

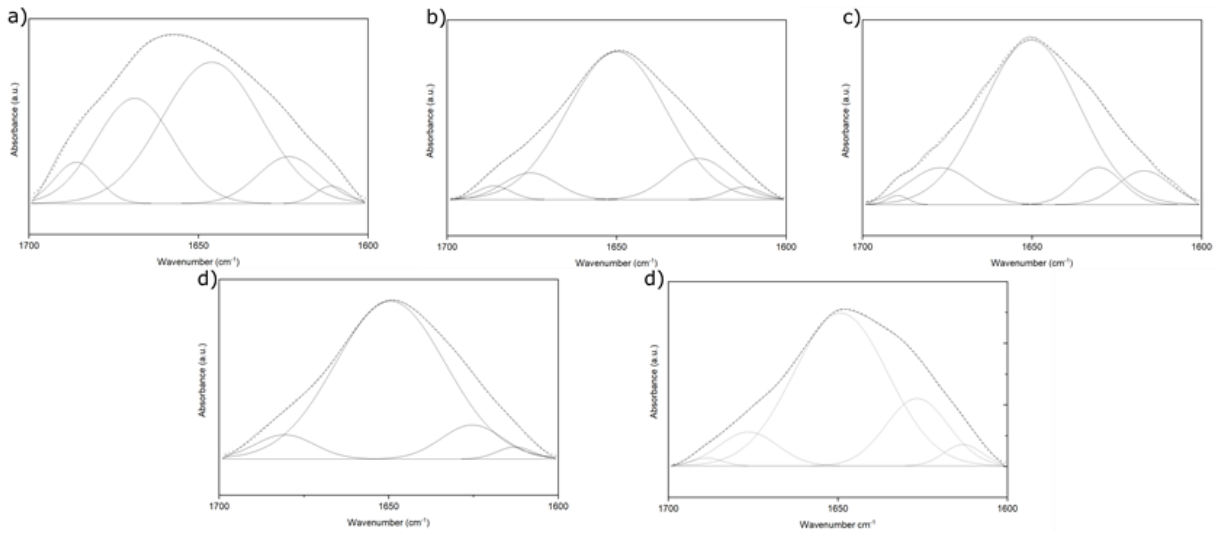

Figure 4. *Amide-I component bands on;* ***a)*** *Ti,* ***b)*** *SB,* ***c)*** *20V,* ***d)*** *40V and* ***e)*** *60V samples*

The extent of changes in the secondary structure of BSA was not directly correlated with the WCA of the surfaces and BSA has undergone significant conformational changes even on the hydrophilic anodized surfaces. It is generally recognized that proteins undergo less denaturation upon adsorption on hydrophilic surfaces and the restriction of protein-surface interactions due to water-surface interactions on hydrophilic

TiO_2 surfaces were reported to cause less denaturation compared to hydrophobic surfaces (Zhao et al., 2020). However, this conclusion doesn't take the effect of surface morphology into consideration. No direct correlation between surface roughness the contents of secondary structure components were observed, but the way in which the secondary structure of BSA was changed was unique on each surface that has different Ra values. In addition, as the surface roughness increased the total α-helix and random helix content of the secondary structure components of BSA increased as well. The position of the amide-I band suggests that this change is the sum of the α-helix content decreasing and random coil content increasing. This finding is in agreement with the literature where a general reduction in α-helix content as a result of adsorption of BSA to hydrophilic surfaces is reported (Giacomelli et al., 1999). Surface roughness can affect how a protein behaves on a surface by influencing the surface hydrophilicity and by increasing the specific surface area with which the protein can interact. In particular, micro-sized roughness increases the surface area and consequently increases the amount of protein adsorption. However, there are conflicting data on the effect of nanometer roughness on protein adsorption. For example, Cai et al. (2006) reported that Ra values between 1.57-16.44 nm affect BSA adsorption to a lesser extent the adsorption of fibrinogen to a greater but a still a limited extent. Rockwell et al. (2012), on the other hand, reported that increased surface curvature increases protein adsorption, and Lu et al. (2012) reported that increasing surface roughness between 1-11 nm increases protein adsorption due to an increase in the surface free energy (Lu et al., 2012). Zhao et al. (2020) reported that upon BSA adsorption on TiO_2 nanofibers, a significant increase in β-turn and β-sheet content was observed while the random coil structure disappeared. The diameters of these structures varied between 184 ± 8 nm and 511 ± 17 nm. They interpreted that the dipole moment provided by the surface OH groups, which are strong enough to disrupt the H bonds in the protein structure, may have been responsible for the formation of a new secondary structure in the protein (Zhao et al., 2020). Yang et al. (2021) investigated the adsorption of globular proteins on smooth and nano-rippled TiOx/Ti and SiOx/Si. They reported that surfaces having less than 2 nm features at the vertical scale can significantly affect the amount protein adsorption and denaturation (Yang et al., 2021). Other researchers reported that for BSA, Ti nanotubes having inner diameters between 32 ± 4-80 ± 7 nm caused increased α-helix and β turn content in smaller pore sizes, while β-layer structure increased with high pore diameters (Jia et al., 2020). Our results are in accordance with Jia et al. (2020); the pore size rather than surface roughness influences the conformation BSA on anodized samples where regular β-sheet structure content increases with increasing pore size (Table 1).

***Table-1**. Secondary structure components of surface adsorbed BSA*

	Ti		**SB**		**20V**		**40V**		**60V**	
Secondary structure	**Wavenumber (cm^{-1})**	**%**	**Wavenumber (cm^{-1})**	**%**	**Wavenumber (cm^{-1})**	**%**	**Wavenumber (cm^{-1})**	**%**	**Wavenumber (cm^{-1})**	**%**
α-helix and random coil	1646	52	1650	77	1650	72	1649	83	1649	69
β-sheet	1623	11	1626	13	1630	8	1625	10	1626	20
β-turns	1669, 1686	37	1675, 1689	10	1677, 1690	13	1681	7	1676, 1688	10
Side chains	1611	-	1613	-	1617	-	1613	-	1613	-

4. CONCLUSION

Our findings can be summarized as follows;

Although sanding increases the surface roughness, it partially improves the surface wettability, while the anodization process significantly increases the surface wettability

BSA undergoes significant conformational changes on all surfaces upon adsorption irrespective of surface hydrophilicity and roughness and the extent of the changes in conformation of BSA is not directly correlated with the surface hydrophilicity and the surface roughness

For anodized samples a correlation between the pore diameter and the secondary structure of surface adsorbed BSA adsorbed was observed.

Our results indicate that the protein adsorption behavior is dependent on nano-morphological features other than the surface roughness.

ACKNOWLEDGEMENT

This study has been funded by Ankara Hacı Bayram Veli University Scientific Research Projects Coordination Centre, Ankara, Turkey (Project No. 01/2020-24). SEM and AFM images and FTIR-ATR spectra were obtained at Hacettepe University, Advanced Technologies Research and Applications Center (HUNITEK), National Nanotechnology Research Center Institute of Materials Science and Nanotechnology (UNAM), and Eastern Anatolia High Technology Application and Research Center (DAYTAM) respectively.

CONFLICT OF INTEREST

The authors declare no conflict of interest.

REFERENCES

Akdoğan, E., & Mutlu, M. (2012). Generation of amphoteric surfaces via glow-discharge technique with single precursor and the behavior of bovine serum albumin at the surface. *Colloids and Surfaces B: Biointerfaces, 89*, 289-294. doi:10.1016/j.colsurfb.2011.09.005

Barberi, J. & Spriano, S. (2021). Titanium and protein adsorption: an overview of mechanisms and effects of surface features. *Materials*, *14*(7), 1590. doi:10.3390/ma14071590

Byler, D. M. & Susi, H. (1986). Examination of the secondary structure of proteins by deconvolved FTIR spectra. *Biopolymer*, *25*(3), 469-487. doi:10.1002/bip.360250307

Cai, K., Bossert, J., & Jandt, K. D. (2006). Does the nanometre scale topography of titanium influence protein adsorption and cell proliferation?. *Colloids and surfaces B: Biointerfaces*, *49*(2), 136-144. doi:10.1016/j.colsurfb.2006.02.016

Chen, X., Chen, J., & Huang, N. (2022). The structure, formation, and effect of plasma protein layer on the blood contact materials: A review. *Biosurface and Biotribology*, *8*(1), 1-14. doi:10.1049/bsb2.12029

Della Porta, V., Bramanti, E., Campanella, B., Tiné, M. R., & Duce, C. (2016). Conformational analysis of bovine serum albumin adsorbed on halloysite nanotubes and kaolinite: A Fourier transform infrared spectroscopy study. *RSC Advances*, *6*(76), 72386-72398. doi:10.1039/C6RA12525E

Gan, N., Peng, X., Wu, D., Xiang, H., Sun, Q., Yi, B., Suo, Z., Zhang, S., Wang, X., & Li, H. (2022). Effects of Micro or Nano Size on the Biocompatibility of UiO67 from Protein Adsorption Behavior, Hemocompatibility and Histological Toxicity. *Journal of Hazardous Materials*, *435*, 129042. doi:10.1016/j.jhazmat.2022.129042

Giacomelli, C. E., Bremer, M. G., & Norde, W. (1999). ATR-FTIR study of IgG adsorbed on different silica surfaces. *Journal of Colloid and Interface Science*, *220*(1), 13-23. doi:10.1006/jcis.1999.6479

Hu, B., Liu, R., Liu, Q., Lin, Z., Shi, Y., Li, J., Wang, L., Li, L., Xiao, X., & Wu, Y. (2022). Engineering surface patterns on nanoparticles: New insights on nano-bio interactions. *Journal of Materials Chemistry B*, *10*(14), 2357-2383. doi:10.1039/D1TB02549J

Qi, H., Shi, M., Ni, Y., Mo, W., Zhang, P., Jiang, S., Zhang, Y., & Deng, X. (2021). Size-Confined Effects of Nanostructures on Fibronectin-Induced Macrophage Inflammation on Titanium Implants. *Advanced Healthcare Materials*, *10*(20), 2100994. doi:10.1002/adhm.202100994

Jia, E., Zhao, X., Lin, Y., & Su, Z. (2020). Protein adsorption on titanium substrates and its effects on platelet adhesion. *Applied Surface Science*, *529*, 146986. doi:10.1016/j.apsusc.2020.146986

La Verde, V., Dominici, P., & Astegno, A. (2017). Determination of hydrodynamic radius of proteins by size exclusion chromatography. *Bio-protocol*, *7*(8), e2230. doi:10.21769/BioProtoc.2230

Li, K., Liu, S., Hu, T., Razanau, I., Wu, X., Ao, H., Huang, L., Xie, Y., & Zheng, X. (2020). Optimized nanointerface engineering of micro/nanostructured titanium implants to enhance cell–nanotopography interactions and osseointegration. *ACS Biomaterials Science & Engineering*, *6*(2), 969-983. doi:10.1021/acsbiomaterials.9b01717

Liu, C., Guo, Y., Hong, Q., Rao, C., Zhang, H., Dong, Y., Huang, L., Lu, X., & Bao, N. (2016). Bovine serum albumin adsorption in mesoporous titanium dioxide: pore size and pore chemistry effect. *Langmuir*, *32*(16), 3995-4003. doi:10.1021/acs.langmuir.5b04496

Lord, M. S., Foss, M., & Besenbacher, F. (2010). Influence of nanoscale surface topography on protein adsorption and cellular response. *Nanotoday*, *5*(1), 66-78. doi:10.1016/j.nantod.2010.01.001

Lu, J., Yao, C., Yang, L., & Webster, T. J. (2012). Decreased platelet adhesion and enhanced endothelial cell functions on nano and submicron-rough titanium stents. *Tissue Engineering Part A*, *18*(13-14), 1389-1398. doi:10.1089/ten.tea.2011.0268

Rockwell, G. P., Lohstreter, L. B., & Dahn, J. R. (2012). Fibrinogen and albumin adsorption on titanium nanoroughness gradients. *Colloids and Surfaces B: Biointerfaces*, *91*, 90-96. doi:10.1016/j.colsurfb.2011.10.045

Singh, A. V., Vyas, V., Patil, R., Sharma, V., Scopelliti, P. E., Bongiorno, G., Podestà, A., Lenardi, C., Gade, W. N., & Milani, P. (2011). Quantitative characterization of the influence of the nanoscale morphology of nanostructured surfaces on bacterial adhesion and biofilm formation. *PloS one*, *6*(9), e25029. doi:10.1371/journal.pone.0025029

Sirin, H. T., Vargel, I., Kutsal, T., Korkusuz, P., & Piskin, E. (2016). Ti implants with nanostructured and HA-coated surfaces for improved osseointegration. *Artificial Cells, Nanomedicine, and Biotechnology*, *44*(3), 1023-1030. doi:10.3109/21691401.2015.1008512

Wu, B., Tang, Y., Wang, K., Zhou, X., & Xiang, L. (2022). Nanostructured Titanium Implant Surface Facilitating Osseointegration from Protein Adsorption to Osteogenesis: The Example of TiO_2 NTAs. *International Journal of Nanomedicine*, *17*, 1865-1879. doi:10.2147/IJN.S362720

Yang, Y., Yu, M., Böke, F., Qin, Q., Hübner, R., Knust, S., Schwiderek, S., Grundmeier, G., Fischer, H., & Keller, A. (2021). Effect of nanoscale surface topography on the adsorption of globular proteins. *Applied Surface Science*, *535*, 147671. doi:10.1016/j.apsusc.2020.147671

Zhao, F. H., Chen, Y. M., Hu, Y., Lu, X. G., Xiong, S. B., Wu, B. Y., Guo, Y. Q., Huang, P., & Yang, B. C. (2020). Conformation changes of albumin and lysozyme on electrospun TiO_2 nanofibers and its effects on MSC behaviors. *Colloids and Surfaces B: Biointerfaces*, *185*, 110604. doi:10.1016/j.colsurfb.2019.110604